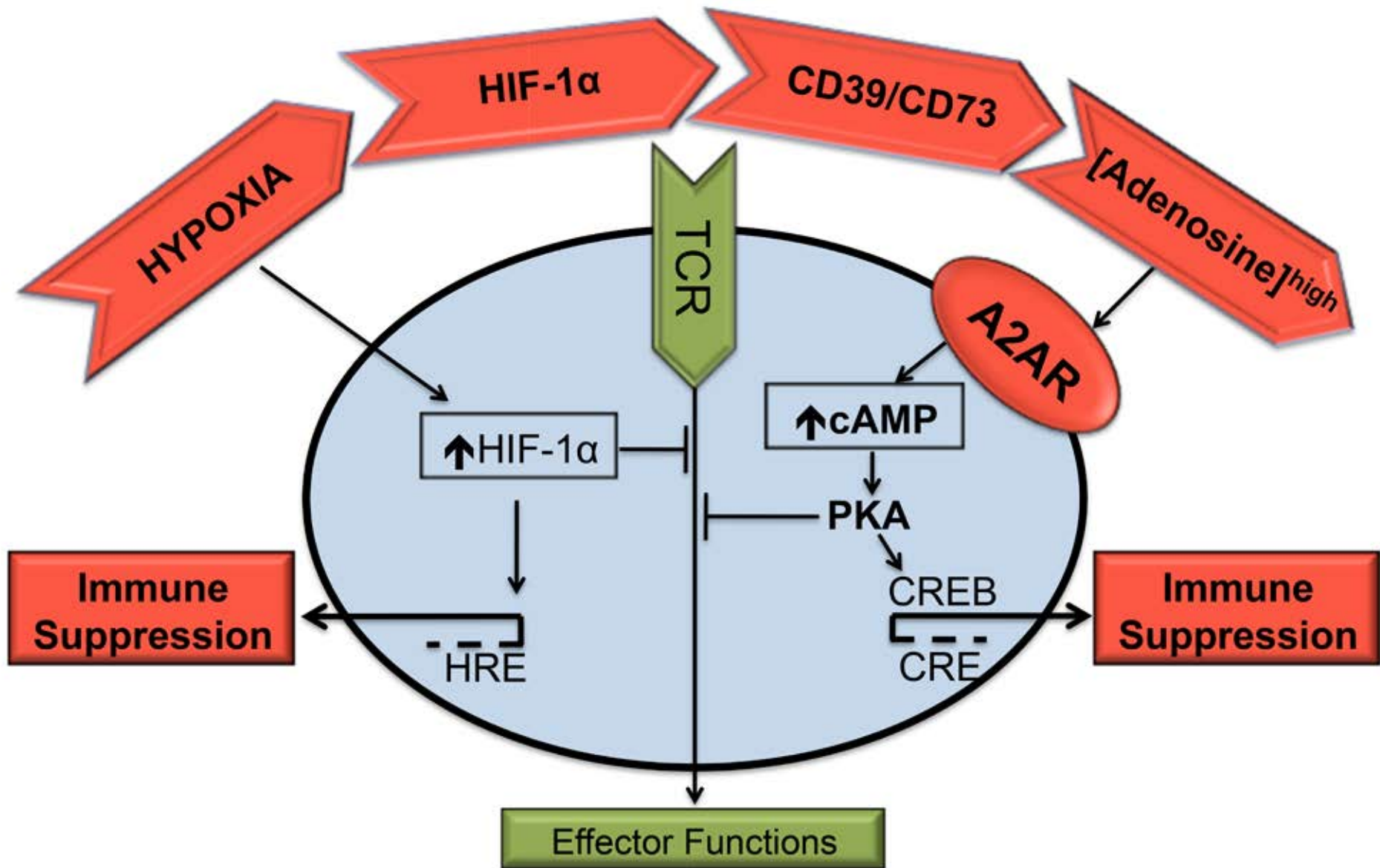


**Systemic oxygenation weakens the hypoxia and Hypoxia Inducible Factor 1 $\alpha$ -dependent and extracellular adenosine-mediated tumor protection**

Stephen M. Hatfield<sup>1</sup>, Jorgen Kjaergaard<sup>1</sup>, Dmitriy Lukashev<sup>1</sup>, Bryan Belikoff<sup>1</sup>, Taylor H. Schreiber<sup>3</sup>, Shalini Sethumadhavan<sup>1</sup>, Robert Abbott<sup>1</sup>, Phaethon Philbrook<sup>1</sup>, Molly Thayer<sup>1</sup>, Dai Shujia<sup>5</sup>, Scott Rodig<sup>4</sup>, Jeffrey L. Kutok<sup>4</sup>, Jin Ren<sup>6</sup>, Akio Ohta<sup>1</sup>, Eckhard R. Podack<sup>3</sup>, Barry Karger<sup>5</sup>, Edwin K. Jackson<sup>6</sup> and Michail Sitkovsky<sup>1,2</sup>



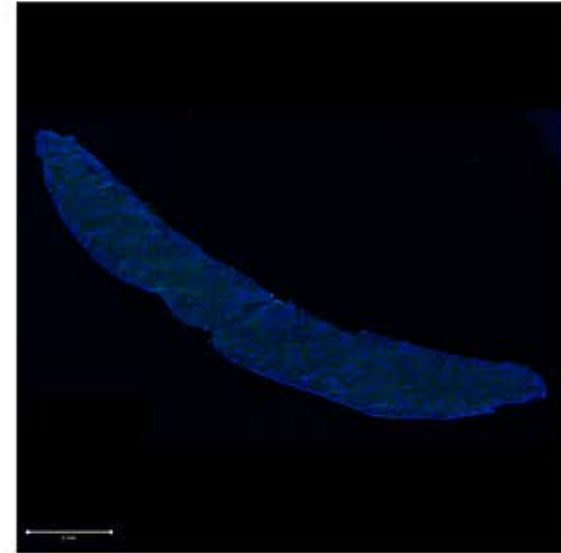
**S1. Mechanistic details of immunosuppression mediated by hypoxia and adenosine signaling.** Schematic of the early stages of Hypoxia→HIF-1alpha signaling that may govern the downstream molecular events of the hypoxia-adenosinergic pathway, i.e. TME hypoxia → HIF-alpha → CD39/CD73 → [Adenosine] → A2AR/A2BR → intracellular cAMP → PKA→ cAMP Response Element (CRE) → CREB pathway. [Abbreviations: PKA (protein kinase A), cAMP (cyclic AMP), CREB (cyclic AMP response element binding protein), CRE (cyclic AMP response element), HRE (hypoxia response element)]

Spleen

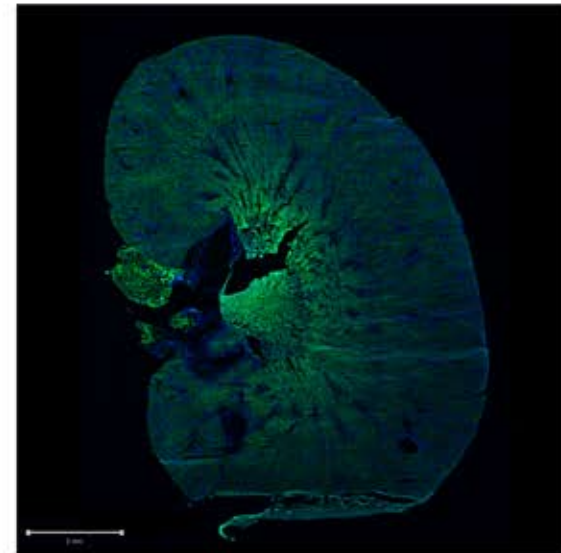
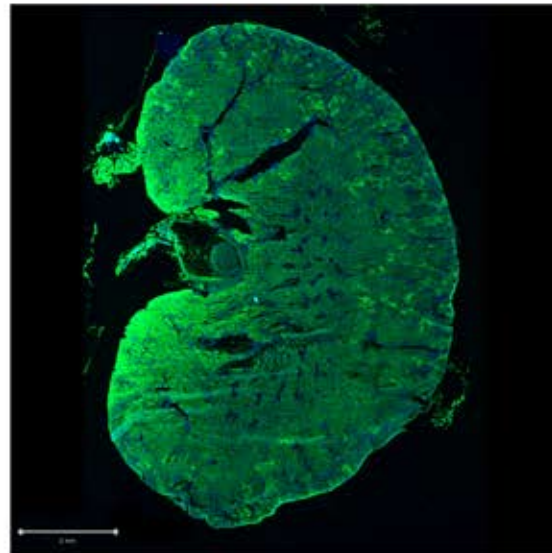
21%



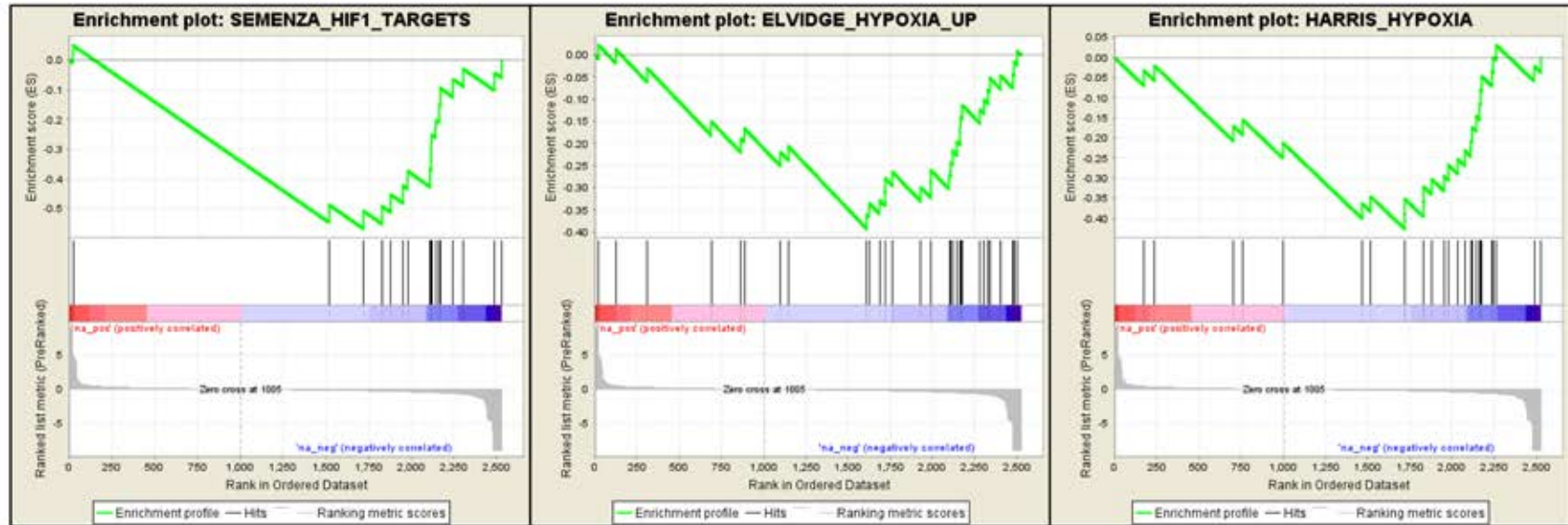
60%



Kidney



**S2. Breathing 60% oxygen reduces inflammatory damage-associated hypoxia in the spleen and kidney of mice with acute microbial sepsis.** Cecal ligation and puncture (CLP) surgery was performed on CD-1 mice prior to exposure to either 21% or 60% oxygen. After 24 h, mice were injected with Hypoxyprobe (1.5 h) and frozen spleen and kidney tissue sections were prepared. Hypoxyprobe staining is shown in green in the fluorescent micrographs. Immunohistochemistry was performed as described in methods; shown are representative images (10x magnification).

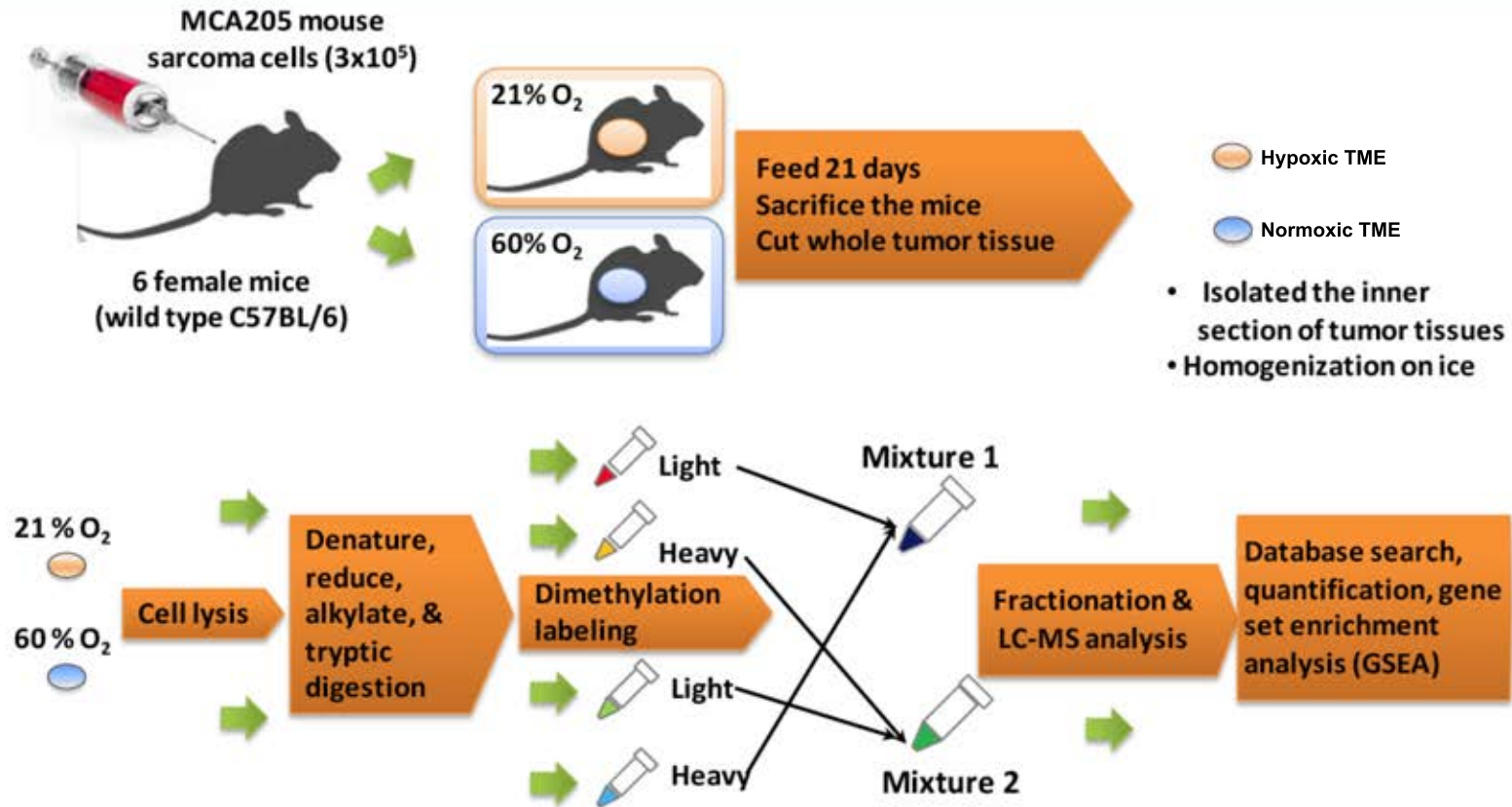
**A****B**

Name	Log2 ratio (60%/21%)	Description
aldoa	-0.371	aldolase A, fructose-bisphosphate
eno1	-0.303	enolase 1, (alpha)
ndrg1	-0.822	N-myc downstream regulated gene 1
aldoc	-0.748	aldolase C, fructose-bisphosphate
tf	-0.483	transferrin
ero1l	-0.539	ERO1-like ( <i>S. cerevisiae</i> )
pfkl	-0.540	phosphofructokinase, liver
pgm1	-0.472	phosphoglucomutase 1
pkm2	-8.966	pyruvate kinase, muscle
gapdh	-0.140	glyceraldehyde-3-phosphate dehydrogenase
tgm2	-0.448	transglutaminase 2 (C polypeptide, protein-glutamine-gamma-glutamyltransferase)
p4ha1	-0.217	procollagen-proline, 2-oxoglutarate 4-dioxygenase (proline 4-hydroxylase), alpha polypeptide I
vim	-0.275	vimentin
tpi1	-0.487	triosephosphate isomerase 1
Ldha	-0.632	lactate dehydrogenase A
pgk1	-0.487	phosphoglycerate kinase 1
ptrf	-1.339	polymerase I and transcript release factor

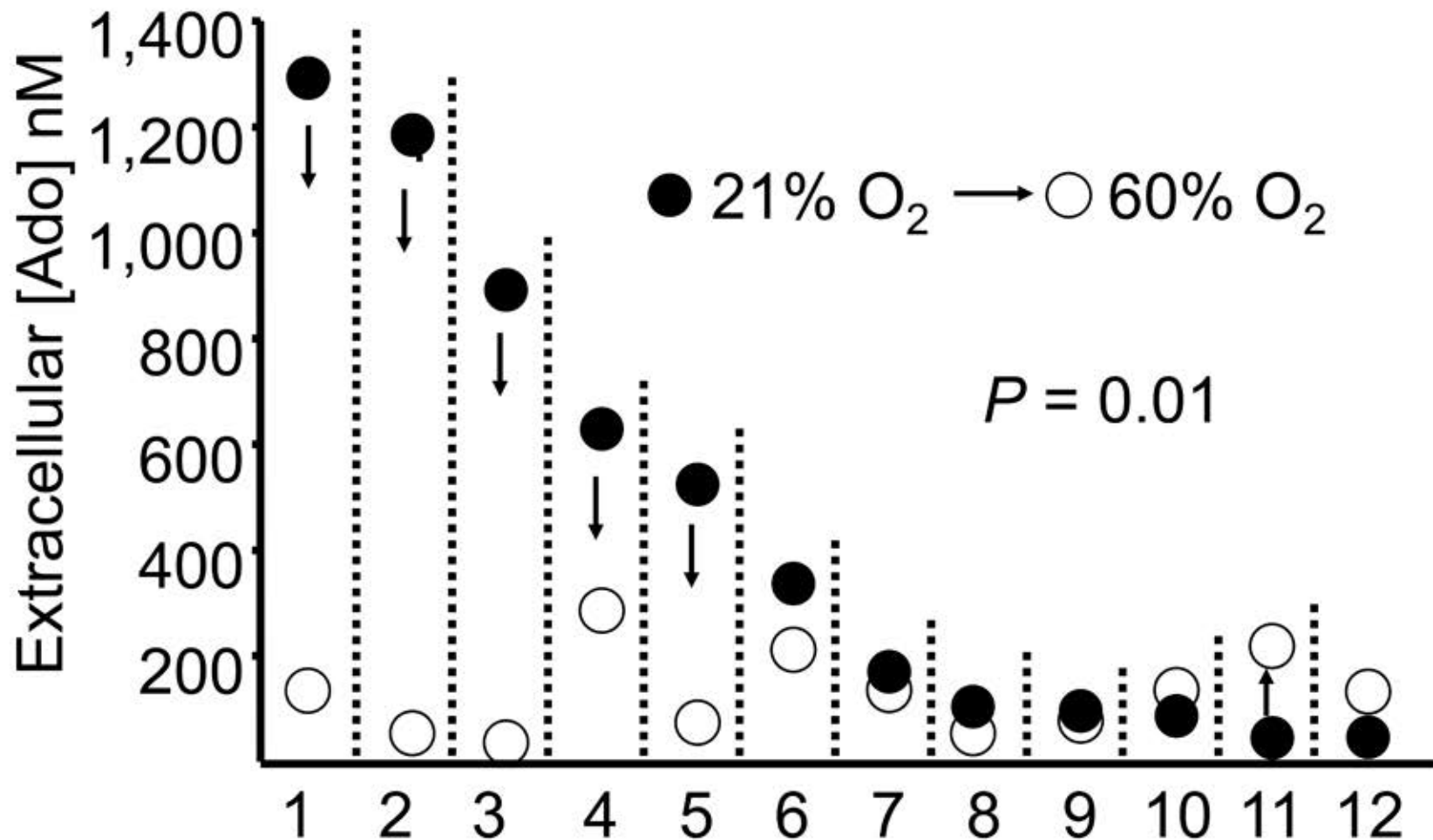
### S3. GSEA analysis of comparative whole cell proteomics demonstrate the downregulation of HIF-1alpha targets in the TME.

(A) The enrichment plots demonstrate graphically the down-regulation of gene sets related to HIF-1alpha/hypoxia. The primary result of the gene set enrichment analysis is the enrichment score (ES), which reflects the degree to which a gene set is overrepresented at the top or bottom of a ranked list of genes. GSEA calculates the ES by walking down the ranked list of genes, increasing a running-sum statistic when a gene is in the gene set and decreasing it when it is not. The magnitude of the increment depends on the correlation of the gene with the phenotype. The ES is the maximum deviation from zero encountered in walking the list. A positive ES indicates gene set enrichment at the top of the ranked list; a negative ES indicates gene set enrichment at the bottom of the ranked list. (B) GSEA results of the downregulation of HIF-alpha regulated proteins.

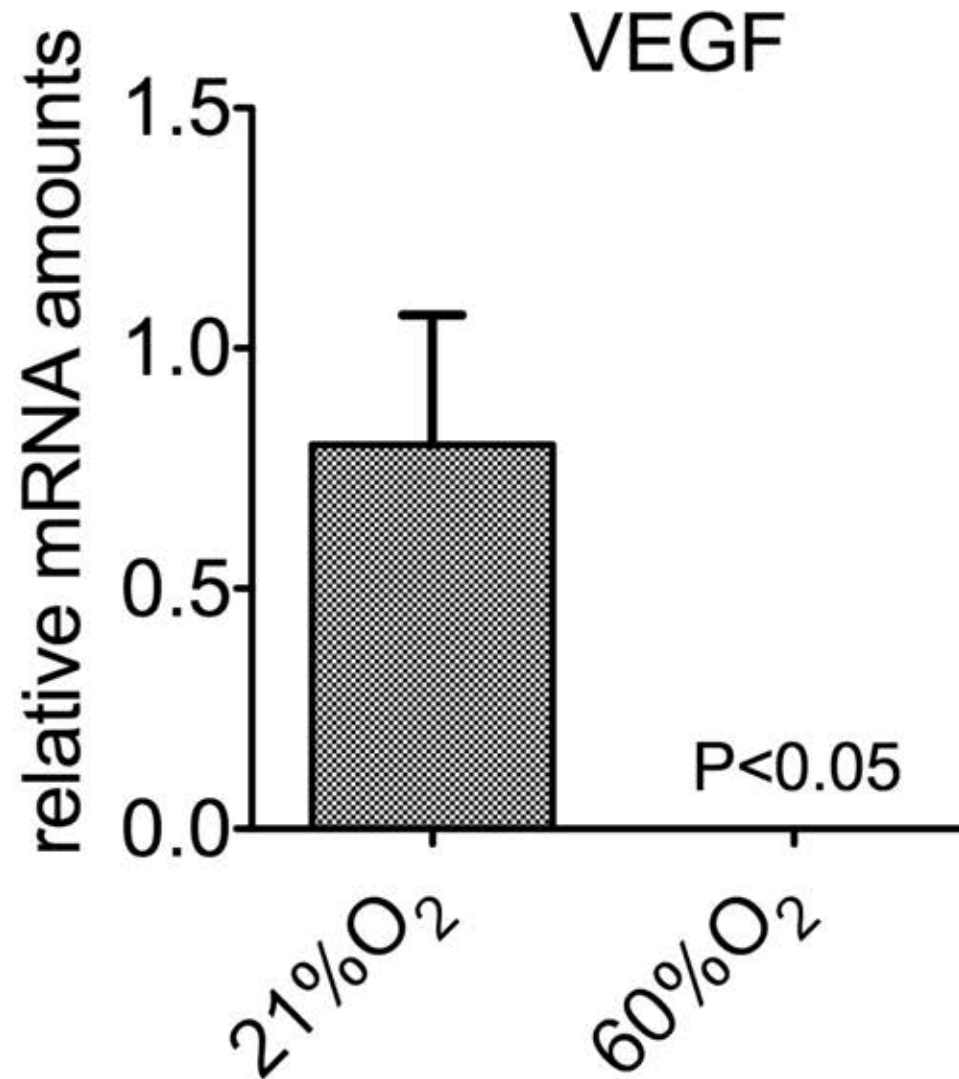
## Schematic Workflow and Design of Experiment



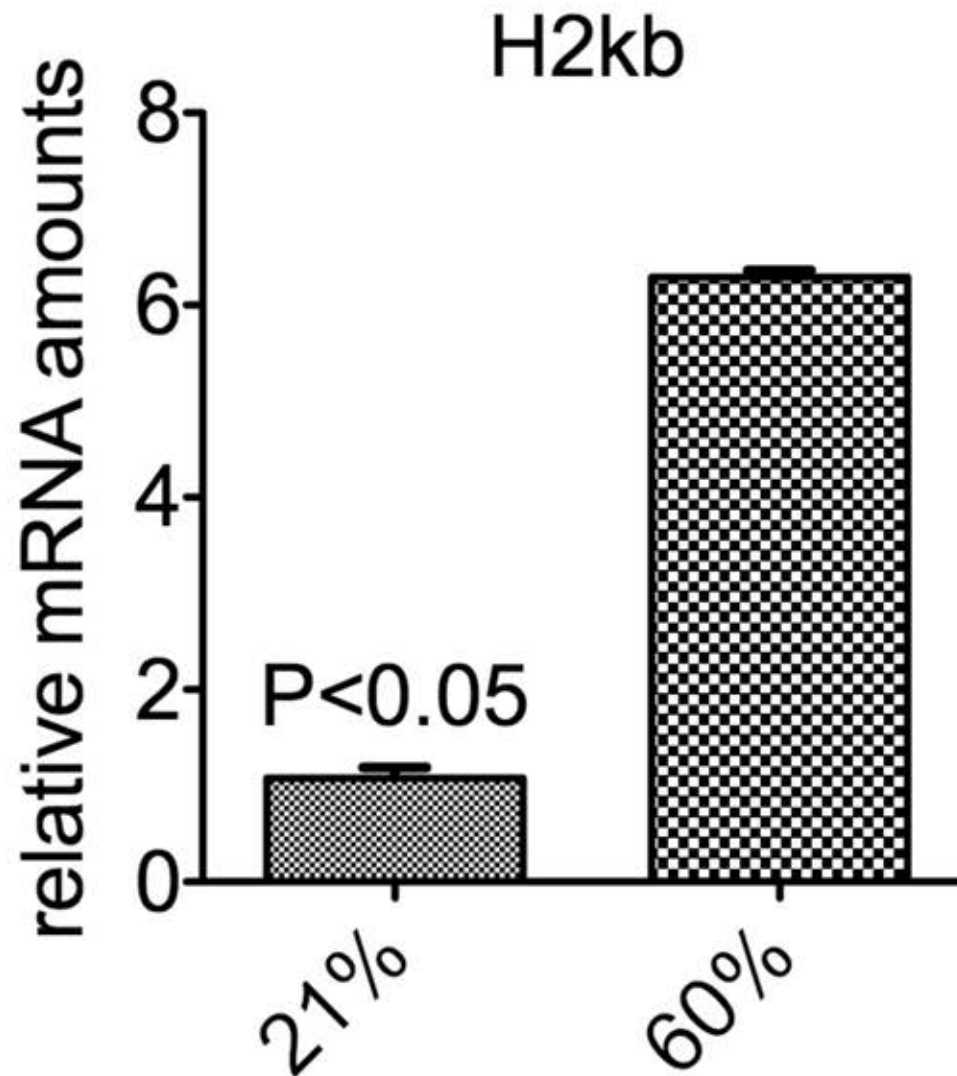
**S4. Work-flow of preparation of samples for analysis of hypoxic vs. normoxic TME in proteomics studies.** The protocols are also described in methods and discussed in (3-6). Mice with established MCA205 fibrosarcoma cells were breathing 21% or 60% oxygen for 14 days. Individual tumors were dissected into 12-15 sections representing different TMEs and extracted for protein analysis. Whole tumor cell extracts from different TMEs were separated by SDS PAGE and then pre-screened for HIF-1 $\alpha$  levels by Western blot to identify (HIF-1 $\alpha$  high) vs. (HIF-1 $\alpha$  low) regions to select samples prior to proteomics analysis. Tumor sections representing hypoxic regions (HIF-1 $\alpha$  high) from mice breathing 21% O<sub>2</sub> were compared to normoxic (HIF-1 $\alpha$  low) regions from tumors of mice breathing 60% oxygen. Each sample was digested by trypsin and labeled with isotope dimethyl reagents. The labeled peptide mixture was then separated by a 2D-RP-RPLC and detected by a Q-Exactive Orbitrap-MS. Proteome Discoverer v1.3 was used for protein identification; the empirical Bayesian analysis for differential quantitation; and the Ingenuity pathway analysis (IPA) for functional analysis. The high performance orthogonal separation combined with the high resolution and accurate mass (HRAM) detection by Q-Exactive Orbitrap MS resulted in the identification of over 6400 mouse proteins at a false discovery rate (FDR) of 1% at the peptide level. About 5200 proteins were quantitated by at least two unique peptides based on the peak area of precursor ions from light/heavy isotope dimethyl labeled peptides from two technical replicates. To avoid the arbitrary cutoff for protein fold changes, an empirical Bayesian analysis was applied to determine the thresholds of significant fold changes and lead to near 1000 differential proteins at an estimated FDR of 5%. These proteins along with their ratios between normoxic and hypoxic tumor microenvironments (TME) were submitted to the IPA software and associated with various molecular functions, biological processes and pathways.



**S5. High levels of intratumoral extracellular adenosine are significantly reduced in mice breathing 60% oxygen.** Levels of extracellular adenosine in different TMEs of intradermal tumors before and after supplemental oxygenation. Mice with established MCA205 tumors breathing ambient oxygen were given an initial probe to collect levels of extracellular adenosine. After equilibration, the same tumor area was re-probed after exposure to either 21% or 60% oxygen for 3 h. The microdialysate was collected and assessed for levels of extracellular adenosine by HPLC/MS. As shown, supplemental oxygenation did not effect adenosine concentration where intratumoral extracellular adenosine levels were already low (< 200 nM) (*P* = 0.01). The protocols of adenosine measurements by HPLC/MS are described in detail in (7-9).



**S6. Breathing 60% oxygen reduces intratumoral expression of VEGF.** Mice bearing established B16 s.c. tumors were placed in 21% or 60% O<sub>2</sub> for 72h, tumors were excised and total RNA was extracted and subjected to RT-qPCR analysis (P < 0.05, n = 3).



**S7. Breathing 60% oxygen increases the intratumoral expression of antigen-presenting MHC class I from B16 tumors.** Mice bearing established B16 s.c. tumors were placed in 21% or 60% O<sub>2</sub> for 72h, tumors were excised and total RNA was extracted and subjected to RT-qPCR analysis ( $P < 0.05$ ,  $n = 3$ ).



## Supplemental Information

### Supplemental Methods

**Tumors.** MCA205 fibrosarcoma is a 3-methylcholanthrene-induced tumor of B6 origin (10, 11); B16-F10.P1 is a poorly immunogenic subclone of the spontaneously arising B16/BL6 melanoma (12); B16-F10.P1 is the parent strain of CL8-1 (transfected with MHC Class I) (13). To establish tumors, B6 mice were injected s.c. ( $1 \times 10^5$ ) or i.v. ( $3 \times 10^5$ ) with tumor cells resuspended in 200  $\mu$ l of HBSS. Mice with subcutaneous tumors were placed in either 21% or 60% oxygen after tumors became palpable (between day 7 and 10). Tumor size was measured in two dimensions using vernier calipers. Protocols of tumor immunology assays are described in detail in (10-13).

**Hyperoxic breathing.** Mice were placed in chambers with well-controlled gas composition to mimic protocols of supplemental oxygen delivery to humans (14). Self-contained oxygen generators (Airsep) were used to ensure desired levels of oxygen were maintained inside each unit. Hypercapnic acidosis was avoided by replacing traditional mouse cage tops with aerated wire lids and by using Sodasorb (Grace&Co) (1, 2). CO<sub>2</sub> levels inside the chamber never exceeded 0.4%, while hypercapnia typically occurs at levels higher than 2%. Confirmation of the levels of CO<sub>2</sub> and O<sub>2</sub> in control and experimental groups treated with 21% or 60% oxygen was done in collaboration with Dr. Richard Marsh, an expert in the field of energetics, kinematics and kinetics. Fractional concentrations of O<sub>2</sub> and CO<sub>2</sub> were monitored by pulling a sample from the chamber at a rate of 100 ml min<sup>-1</sup> using a Sable Systems Model SS3 sample pump (Sable Systems, Las Vegas, NV). The gas sample was pulled in order through: 1) a column of Drierite to remove water vapor; 2) a Sable Systems Model CA-1 CO<sub>2</sub> analyzer to measure the fractional concentration of CO<sub>2</sub>; and 3) a Sable Systems Model FC-10 O<sub>2</sub> analyzer to measure the fractional concentration of O<sub>2</sub>. The O<sub>2</sub> analyzer was calibrated using dry, CO<sub>2</sub> air that was assumed to be 20.95% oxygen, and the CO<sub>2</sub> analyzer was calibrated using a 5.0 % calibration gas from Medical-Technical Gases (North Billerica, MA). Analog signals from the gas analyzers were recorded on a Macintosh Computer using a 16-bit A-D converter (AD Instruments Model Sp16, Colorado Springs, CO) and the application LabChart from AD Instruments.

**Immunohistochemistry.** Immunohistochemistry was performed at Harvard Medical School Pathology Department at Brigham and Women's Hospital. Four micrometer thick acetone-fixed, O.C.T-embedded tissue sections were prepared. The slides were soaked in -20°C methanol-acetic acid for 2 min then air-dried for 20 min at room temperature. Slides were pre-treated with Peroxidase Block (DAKO). Primary anti-Hypoxypore (Millipore) was applied at a concentration of 1:100 at room temperature for 1h. Rabbit anti-rat immunoglobulin antibody was applied at a concentration of 1:750 in DAKO diluent for 1h. Slides were detected with anti-rabbit Envision+ kit (DAKO). Immunoperoxidase staining was developed using a DAB chromogen (DAKO) and counterstained with hematoxylin. Tumor hypoxia was annotated using Spectrum™ Plus and Aperio's ScanScope® slide scanners by the Pathology Department at Brigham and Women's Hospital.

For fluorescence staining, sections were fixed in 1:1 acetone/methanol solution and incubated with Fc-block (CD16/32) followed by phycoerythrin conjugated VEGF-R (CD309) (Ebiosciences) or PECAM-1 (CD31) (BD Pharmingen) antibodies diluted at 1:200 for 3 hours. The slides were washed and stained with DAPI at a concentration of 300 nm (Invitrogen). The mean integrated optical density was quantified and normalized to tumor area in > 60 different tumors per group from 10-20 different cutting sections using ImageJ software (NIH, MacBioPhotonics). Fluorescent Hypoxypore staining in septic mice was carried out using anti-Hypoxypore FITC (clone 4.3.11.3, Millipore) monoclonal antibody at a dilution of 1:200 and analyzed on a Zeiss LSM 710 confocal microscope.

**Whole cell proteomics.** Mice bearing 7-day established MCA205 intradermal tumors were placed in either 21% or 60% oxygen. On day 21, tumors were excised and homogenized in protein extraction lysing buffer as recommended by manufacturer (Thermo Fisher Scientific). After denaturing and enzymatic digestion by trypsin, the 21% O<sub>2</sub> and 60% O<sub>2</sub> samples were labeled with differential stable-isotopic labeling using dimethylation reaction (15) A two-dimensional HPLC separation was performed by high/low pH reverse phase HPLC24 and a Q-Exactive Orbitrap mass spectrometer (Thermo Fisher Scientific) to acquire the MS and MS/MS spectra of isotopically labeled

peptide signals. Leading edge analysis using GSEA software showed that five gene sets were highly correlated with the observed HIF- $\alpha$  regulated proteins. Only those protein sets that fall into  $< 0.25$  false discovery rate (FDR) and were significant in the GSEA output are shown below.

Tumors were solubilized in ice-cold homogenization buffer (0.32 M sucrose, 10 mM Hepes, 1 mM EDTA supplemented with protease inhibitors mixture (Roche) and Phosphatase Inhibitor Cocktail 1 and 2 (Sigma) with Pyrex Potter-Elvehjem Tissue Grinders for 20 times on ice and then added lysis buffer (1 % NP-40, 50mM Tris-HCl, 150 mM NaCl, 5mM EDTA + protease inhibitors mixture (Roche) and Phosphatase Inhibitor Cocktail 1 and 2 (Sigma) to the plate on ice for 1 hour. Unbroken cells and cell debris were cleared by centrifugation at 21,000 x g at 4° C for 20 minutes and preceded to measurement of protein by BCA assay (Pierce, Rockford, IL).

Each sample was digested by trypsin and labeled with isotope dimethyl reagents. The labeled peptide mixture was then separated by a 2D-RP-RPLC and detected by a Q-Exactive Orbitrap-MS. Proteome Discoverer v1.3 was used for protein identification; the empirical Bayesian analysis for differential quantitation; and the Ingenuity pathway analysis (IPA) for functional analysis. The high performance orthogonal separation combined with the high resolution and accurate mass (HRAM) detection by Q-Exactive Orbitrap MS resulted in the identification of over 6400 mouse proteins at a false discovery rate (FDR) of 1 % at the peptide level. About 5200 proteins were quantitated by at least two unique peptides based on the peak area of precursor ions from light/heavy isotope dimethyl labeled peptides from two technical replicates. To avoid the arbitrary cutoff for protein fold changes, an empirical Bayesian analysis was applied to determine the thresholds of significant fold changes and lead to near 1000 differential proteins at an estimated FDR of 5%. These proteins along with their ratios between hyperoxic and hypoxic tumor microenvironments (TME) were submitted to the IPA software and associated with various molecular functions, biological processes and pathways. Additional details on proteomic analysis are found in (3-6).

In assays to identify proteins that were upregulated specifically in hypoxic versus normoxic areas, individual tumors were dissected into 12-15 sections and screened by

western blot prior to proteomics analysis. Tumor sections representing hypoxic regions (HIF-1a<sup>high</sup>) from mice breathing 21% O<sub>2</sub> was compared to normoxic (HIF-1a<sub>low</sub>) regions of the TME normalized by 60% oxygen breathing.

**Western blot.** Tumors were solubilized with lysis buffer containing 1% Triton X-100, 50 mmol/l Tris-HCl pH 7.6, 150 mmol/l NaCl, 5mmol/l EDTA, 5 umol/l MG132 (26S proteasome inhibitor), and protease inhibitors cocktail (Pierce, Rockford, IL) on ice for 30 minutes. Lysate was cleared by centrifugation at 20,000 g for 30 minutes and subjected to 7% NuPage Tris-Acetate gel analysis. Semi-wet transfer to the nitrocellulose membrane (Invitrogen) using XCell II Blot Module (Invitrogen) was used to achieve the most efficient transfer of high molecular weight proteins. Antibodies against HIF-1alpha-HRP (Novex, Littleton, CO), FHL-1 at a 1/500 dilution, or beta-actin (Sigma-Aldrich) at a 1/5000 dilution were used in combination with HRP-conjugated goat anti-mouse Ab (Santa Cruz Biotechnology, Santa Cruz, CA) at a 1/5000 dilution before detection using SuperSignal Substrate (Pierce).

**In vivo extracellular adenosine measurements.** Mice with established MCA205 tumors were used to analyze levels of extracellular adenosine. Microdialysis probes (Bioanalytical Systems) were placed in the center, edge and in normal tissue next to tumors. Microdialysate (isotonic saline, 100 U of heparin, and 20 mM EHNA adenosine deaminase inhibitor) was perfused at 2 mL/min for 2.5h using an infusion pump (Braintree Scientific). Following the initial probe and equilibration, mice were placed in 21% or 60% oxygen for 3h and re-probed for levels of adenosine in the same tumor area. Adenosine levels were measured by reversed-phase liquid chromatography-tandem mass spectrometry using a triple quadrupole mass spectrometer with <sup>13</sup>C<sup>10</sup>-adenosine as an internal standard (7-9).

**Cytotoxicity Assay.** MCA205 cells were cultured in 21% oxygen or 60% oxygen for 4 days *in vitro*. Cells were collected by trypsinization and labeled with 100 μCi sodium chromate (Amersham Biosciences) per 2 × 10<sup>6</sup> cells for 1h at 37°C. *In vitro* activated T cells from the tumor draining lymph nodes of MCA205 inoculated mice were used as effector cells and seeded into 96-well round-bottomed plates at the indicated effector/target (E/T) ratios. <sup>51</sup>Cr-labeled MCA-205 cells at 1 × 10<sup>4</sup> cells per well were

used as target cells. After 4 hrs of incubation at 37°C and 5% CO<sub>2</sub>, radioactivity released from lysed target cells was counted on a  $\gamma$ -counter. Percent Specific Lysis was calculated using the following formula:

Percent specific lysis = 100 \* (Experimental release – spontaneous release)/ (Maximum release– spontaneous release). Spontaneous release was calculated from the supernatant of the target cells alone, and the maximum release was obtained by adding 1 M HCl to target cells. The data are expressed as a mean value of triplicate wells.

**Cecal Ligation and Puncture.** CLP was performed as previously described [16-18]. Briefly, mice were anesthetized with 5% isoflourane for induction and 3% for maintenance. Mice abdomens were shaved and disinfected with both alcohol and povidone iodine. The peritoneal cavity was entered through a 2 cm midline laparotomy exposing the cecum. Fifty percent of the cecum was ligated distal to the ileocecal valve in order to prevent bowel obstruction. The cecum was perforated with a single puncture using a 16-gauge needle (BD Biosciences, San Jose, CA, USA). A small amount of feces (5 mm) was manually extruded from the perforation site into the peritoneal cavity. The punctured cecum was then reintroduced into the abdominal cavity and the peritoneum was sutured. Vetbound Tissue Adhesive surgical glue was used to seal the dermal layers. Immediately following surgery mice were given intraperitoneal administration of Buprenex (0.1mg/kg).

### Supplemental Information References

1. Ooi H, *et al.* (2000) Chronic hypercapnia inhibits hypoxic pulmonary vascular remodeling. *Am J Physiol Heart Circ Physiol* 278(2):H331-338.
2. De Smet HR, Bersten AD, Barr HA, & Doyle IR (2007) Hypercapnic acidosis modulates inflammation, lung mechanics, and edema in the isolated perfused lung. *J Crit Care* 22(4):305-313.
3. Dowell JA, Frost DC, Zhang J, & Li L (2008) Comparison of two-dimensional fractionation techniques for shotgun proteomics. *Anal Chem* 80(17):6715-6723.
4. Subramanian A, *et al.* (2005) Gene set enrichment analysis: a knowledge-based approach for interpreting genome-wide expression profiles. *Proc Natl Acad Sci U S A* 102(43):15545-15550.
5. Mootha VK, *et al.* (2003) PGC-1alpha-responsive genes involved in oxidative phosphorylation are coordinately downregulated in human diabetes. *Nat Genet* 34(3):267-273.

6. Margolin AA, *et al.* (2009) Empirical Bayes analysis of quantitative proteomics experiments. *PLoS One* 4(10):e7454.
7. Ren J, Mi Z, & Jackson EK (2008) Assessment of nerve stimulation-induced release of purines from mouse kidneys by tandem mass spectrometry. *J Pharmacol Exp Ther* 325(3):920-926.
8. Ren J, Mi Z, Stewart NA, & Jackson EK (2009) Identification and quantification of 2',3'-cAMP release by the kidney. *J Pharmacol Exp Ther* 328(3):855-865.
9. Jackson EK, Mi Z, Zacharia LC, Tofovic SP, & Dubey RK (2007) The pancreatohepatorenal cAMP-adenosine mechanism. *J Pharmacol Exp Ther* 321(2):799-809.
10. Kjaergaard J & Shu S (1999) Tumor infiltration by adoptively transferred T cells is independent of immunologic specificity but requires down-regulation of L-selectin expression. *J Immunol* 163(2):751-759.
11. Kjaergaard J, Peng L, Cohen PA, & Shu S (2003) Therapeutic efficacy of adoptive immunotherapy is predicated on in vivo antigen-specific proliferation of donor T cells. *Clin Immunol* 108(1):8-20.
12. Yang Q, *et al.* (2006) Morphological appearance, content of extracellular matrix and vascular density of lung metastases predicts permissiveness to infiltration by adoptively transferred natural killer and T cells. *Cancer Immunol Immunother* 55(6):699-707.
13. Ohta A, *et al.* (2006) A2A adenosine receptor protects tumors from antitumor T cells. *Proc Natl Acad Sci U S A* 103(35):13132-13137.
14. Thiel M, *et al.* (2005) Oxygenation inhibits the physiological tissue-protecting mechanism and thereby exacerbates acute inflammatory lung injury. *PLoS Biol* 3(6):e174.
15. Boersema PJ, Raijmakers R, Lemeer S, Mohammed S, & Heck AJ (2009) Multiplex peptide stable isotope dimethyl labeling for quantitative proteomics. *Nat Protoc* 4(4):484-494.
16. Belikoff BG, Hatfield S, Georgiev P, Ohta A, Lukashev D, Buras JA, Remick DG, Sitkovsky M (2011) A2B adenosine receptor blockade enhances macrophage-mediated bacterial phagocytosis and improves polymicrobial sepsis survival in mice. *J Immunol* 186: 2444-2453. DOI 10.4049/jimmunol.1001567  
jimmunol.1001567 [pii]
17. Belikoff B, Hatfield S, Sitkovsky M, Remick DG (2011) Adenosine negative feedback on A2A adenosine receptors mediates hyporesponsiveness in chronically septic mice. *Shock* 35: 382-387. DOI 10.1097/SHK.0b013e3182085f12
18. Georgiev P, Belikoff BG, Hatfield S, Ohta A, Sitkovsky MV, Lukashev D (2013) Genetic deletion of the HIF-1alpha isoform I.1 in T cells enhances antibacterial immunity and improves survival in a murine peritonitis model. *Eur J Immunol* 43: 655-666. DOI 10.1002/eji.201242765